OPEN ACCESS Freely available online

PLOS | COMPUTATIONAL BIOLOGY

Agent-Based Modeling of Oxygen-Responsive Transcription Factors in *Escherichia coli*

Hao Bai[1☯]*, Matthew D. Rolfe[2☯], Wenjing Jia[2], Simon Coakley[1], Robert K. Poole[2], Jeffrey Green[2]*, Mike Holcombe[1]

1 Department of Computer Science, University of Sheffield, Sheffield, United Kingdom, **2** Department of Molecular Biology and Biotechnology, University of Sheffield, Sheffield, United Kingdom

Abstract

In the presence of oxygen (O_2) the model bacterium *Escherichia coli* is able to conserve energy by aerobic respiration. Two major terminal oxidases are involved in this process - Cyo has a relatively low affinity for O_2 but is able to pump protons and hence is energetically efficient; Cyd has a high affinity for O_2 but does not pump protons. When *E. coli* encounters environments with different O_2 availabilities, the expression of the genes encoding the alternative terminal oxidases, the *cydAB* and *cyoABCDE* operons, are regulated by two O_2-responsive transcription factors, ArcA (an indirect O_2 sensor) and FNR (a direct O_2 sensor). It has been suggested that O_2-consumption by the terminal oxidases located at the cytoplasmic membrane significantly affects the activities of ArcA and FNR in the bacterial nucleoid. In this study, an agent-based modeling approach has been taken to spatially simulate the uptake and consumption of O_2 by *E. coli* and the consequent modulation of ArcA and FNR activities based on experimental data obtained from highly controlled chemostat cultures. The molecules of O_2, transcription factors and terminal oxidases are treated as individual agents and their behaviors and interactions are imitated in a simulated 3-D *E. coli* cell. The model implies that there are two barriers that dampen the response of FNR to O_2, i.e. consumption of O_2 at the membrane by the terminal oxidases and reaction of O_2 with cytoplasmic FNR. Analysis of FNR variants suggested that the monomer-dimer transition is the key step in FNR-mediated repression of gene expression.

Citation: Bai H, Rolfe MD, Jia W, Coakley S, Poole RK, et al. (2014) Agent-Based Modeling of Oxygen-Responsive Transcription Factors in *Escherichia coli*. PLoS Comput Biol 10(4): e1003595. doi:10.1371/journal.pcbi.1003595

Editor: Feilim Mac Gabhann, Johns Hopkins University, United States of America

Received July 12, 2013; **Accepted** March 14, 2014; **Published** April 24, 2014

Funding: This work was supported by the Biotechnology and Biological Sciences Council UK through the SysMO initiative and project grant BB/I004122/1. The funders had no role in study design, data collection and analysis, decision to publish, or preparation of the manuscript.

Competing Interests: The authors have declared that no competing interests exist.

* E-mail: hao.bai@sheffield.ac.uk (HB); jeff.green@sheffield.ac.uk (JG)

☯ These authors contributed equally to this work.

Introduction

The bacterium *Escherichia coli* is a widely used model organism to study bacterial adaptation to environmental change. As an enteric bacterium, *E. coli* has to cope with an O_2-starved niche in the host and an O_2-rich environment when excreted. In order to exploit the energetic benefits that are conferred by aerobic respiration, *E. coli* has two major terminal oxidases: cytochrome *bd*-I (Cyd) and cytochrome *bo′* (Cyo) that are encoded by the *cydAB* and *cyoABCDE* operons, respectively [1,2]. Cyd has a high affinity for O_2 and is induced at low O_2 concentrations (micro-aerobic conditions), whereas Cyo has a relatively low affinity for O_2 and is predominant at high O_2 concentrations (aerobic conditions) [3]. These two terminal oxidases contribute differentially to energy conservation because Cyo is a proton pump, whereas Cyd is not [1,2]; however, the very high affinity of Cyd for O_2 allows the bacterium to maintain aerobic respiration at nanomolar concentrations of O_2, thereby maintaining aerobic respiratory activity rather than other, less favorable, metabolic modes [4–6].

The transcription factors, ArcA and FNR, regulate *cydAB* and *cyoABCDE* expression in response to O_2 supply [7]. FNR is an iron-sulfur protein that senses O_2 in the cytoplasm [8,9]. In the absence of O_2 the FNR iron-sulfur cluster is stable and the protein forms dimers that are competent for site-specific DNA-binding and regulation of gene expression [10]. The FNR iron-sulfur cluster reacts with O_2 in such a way that the DNA-binding dimeric form of FNR is converted into a non-DNA-binding monomeric species [10]. Under anaerobic conditions, FNR acts as a global regulator in *E. coli* [11–13], including the *cydAB* and *cyoABCDE* operons, which are repressed by FNR when the O_2 supply is restricted [7]. Under aerobic conditions, repression of *cydAB* and *cyoABCDE* is relieved and Cyd and Cyo proteins are synthesized [3]. In contrast, ArcA responds to O_2 availability indirectly via the membrane-bound sensor ArcB. In the absence of O_2 ArcB responds to changes in the redox state of the electron transport chain and the presence of fermentation products by autophosphorylating [14–16]. Phosphorylated ArcB is then able to transfer phosphate to the cytoplasmic ArcA regulator (ArcA~P), which then undergoes oligomerization to form a tetra-phosphorylated octomer that is capable of binding at multiple sites in the *E. coli* genome [17,18], including those in the promoter regions of *cydAB* and *cyoABCDE* to enhance synthesis of Cyd and inhibit production of Cyo [7,17]. Because the terminal oxidases (Cyd and Cyo) consume O_2 at the cell membrane, a feedback loop is formed that links the activities of the oxidases to the regulatory activities of ArcA and FNR (Figure 1). These features of the system -

Author Summary

The model bacterium *Escherichia coli* has a modular electron transport chain that allows it to successfully compete in environments with differing oxygen (O_2) availabilities. It has two well-characterized terminal oxidases, Cyd and Cyo. Cyd has a very high affinity for O_2, whereas Cyo has a lower affinity, but is energetically more efficient. Expression of the genes encoding Cyd and Cyo is controlled by two O_2-responsive regulators, ArcBA and FNR. However, it is not clear how O_2 molecules enter the *E. coli* cell and how the locations of the terminal oxidases and the regulators influence the system. An agent-based model is presented that simulates the interactions of O_2 with the regulators and the oxidases in an *E. coli* cell. The model suggests that O_2 consumption by the oxidases at the cytoplasmic membrane and by FNR in the cytoplasm protects FNR bound to DNA in the nucleoid from inactivation and that dimerization of FNR in response to O_2 depletion is the key step in FNR-mediated repression. Thus, the focus of the agent-based model on spatial events provides information and new insight, allowing the effects of dysregulation of system components to be explored by facile addition or removal of agents.

combining direct and indirect O_2 sensing with ArcA~P and FNR repression of *cyoABCDE*, and ArcA~P activation and FNR repression of *cydAB* - result in maximal Cyd production when the O_2 supply is limited (micro-aerobic conditions) and maximal Cyo content when O_2 is abundant (aerobic conditions) [3].

Although the cellular locations of the relevant genes (*cydAB* and *cyoABCDE*), the regulators (ArcBA and FNR) and the oxidases (Cyd and Cyo) are likely to be fundamentally important in the regulation of this system, the potential significance of this spatial organization has not been investigated. Therefore, a detailed agent-based model was developed to simulate the interaction between O_2 molecules and the electron transport chain components, Cyd and Cyo, and the regulators, FNR and ArcBA, to shed new light on individual events within local spatial regions that could prove to be important in regulating this core component of the *E. coli* respiratory process.

Results/Discussion

The starting point for this work was the suggestion that spatial effects play an important role in controlling the response of the *E. coli* transcription factor FNR to changes in O_2 availability [15]. Early work showed that when dissolved O_2 was detectable in the culture medium the activity of FNR decreased, exhibiting ~50% activity in the range 2–5 μM dissolved O_2 and that under these conditions the external concentration of O_2 was equivalent to that in the bacterial cytoplasm [19,20]. However, when the cultures were supplied with low concentrations of O_2 in the input gas, dissolved O_2 in the culture medium could not be measured conventionally, because the O_2 is consumed by the respiratory activity of the bacteria. Therefore, a physiological measure of O_2 availability (the aerobiosis scale) was adopted to investigate the effects of low O_2 concentrations on bacteria [21]. On the aerobiosis scale, the minimum O_2 input that results in undetectable excretion of the fermentation product acetate under carbon-limiting conditions is defined as 100% aerobiosis (100% AU). As the amount of O_2 supplied to cultures decreases the specific rate of acetate production (q_{acetate}) increases to a maximum under anaerobic conditions (0% AU). Between these limits (0–100% AU) lies the micro-aerobic range, defined by the linear decrease in q_{acetate} as the O_2 transfer rate increases, i.e. there is an inverse correlation between q_{acetate} and aerobiosis [21]. When the O_2 supply exceeds the minimum required to abolish acetate excretion the AU value extends beyond 100%, reaching 217% when the culture medium is O_2 saturated. This physiological measurement of O_2 availability is reliable for cultures grown at values as low as 4% AU [21]. In previous experiments using this approach steady-state chemostat cultures were established at fixed points on the aerobiosis scale and samples were taken for measurement of the numbers of Cyd and Cyo molecules per bacterial cell (Table 1) [3]. In addition, Western blotting showed that the concentration of FNR in the cell was constant at 3000 protomers per bacterium across the aerobiosis scale (Table 1).

The agent-based model was constructed to simulate interactions between three groups of agents: O_2 molecules, terminal oxidases, (Cyd and Cyo) and regulators (FNR and ArcBA), which interact with O_2 directly or indirectly. As shown in Figure 2, the initial state of the model is defined in the file 0.xml, which contains information on agent properties such as Id, type, status, position etc. – the data in Table 1 was used to provide numbers of Cyd, Cyo, ArcA and FNR molecules. There is no information available on the abundance of ArcB in the cell and thus it was assumed that there are 1000 ArcB molecules per cell based on the ~10:1 ratio of response-regulator to sensor kinase of another *E. coli* two-component system, PhoBR [22]. At the beginning of the simulation, the 0.xml file is read to establish the 3-D *E. coli* cell. From the initial state, the agents start moving randomly within their 3-D activity space, and interact with each other according to a set of pre-defined interaction rules and interaction radii (Tables 2 and 3), leading to an emergent state.

The algorithm of supplying O_2 to the cell responds to given AU levels and automatically calculates the rate of O_2 molecules supplied to the cell. Whilst the model runs, agent information is updated and stored as a series of XML files for further analysis and visualization.

Modeling the regulatory response to O_2 availability

The dynamics of the system were investigated by running the simulation through two cycles of transitions from 0–217% AU. Figure 3a shows a top view of a 3-D *E. coli* cell at 0% AU (steady-state anaerobic conditions). Under these conditions, the FNR molecules are present as dimers, all ArcB molecules are phosphorylated and the ArcA is octameric. The DNA binding sites for ArcA (120 in the model) and FNR (350 in the model) in the nucleoid are fully occupied. The number of ArcA sites was chosen from the data reported by Liu and De Wulf [18]. The model must include a mechanism for ArcA~P to leave regulated promoters. Upon introduction of O_2 into anaerobic steady-state chemostat cultures ~5 min was required to inactivate ArcA-mediated transcription [15]. In the agent-based model presented here, each iteration represents 0.2 sec. Therefore, assuming that ArcA~P leaving the 120 DNA sites is a first order process, then $t_{½}$ is ~45 sec, which is equivalent to ~0.3% ArcA~P leaving the DNA per iteration (Table 3). The number of FNR binding sites was based on ChIP-seq and ChIP-Chip measurements, which detected ~220 FNR sites and a genome sequence analysis that predicted ~450 FNR sites; thus a mid-range value of 350 was chosen [23–25]. Interaction with O_2 causes FNR to dissociate from the DNA (Table 3). Under fully aerobic conditions (217% AU) the FNR dimers are disassembled to monomers, and the different forms of ArcA coexist (Figure 3b). The ArcA- and FNR-DNA binding sites in the nucleoid are mostly unoccupied due to the lower concentrations of FNR dimers and ArcA octamers.

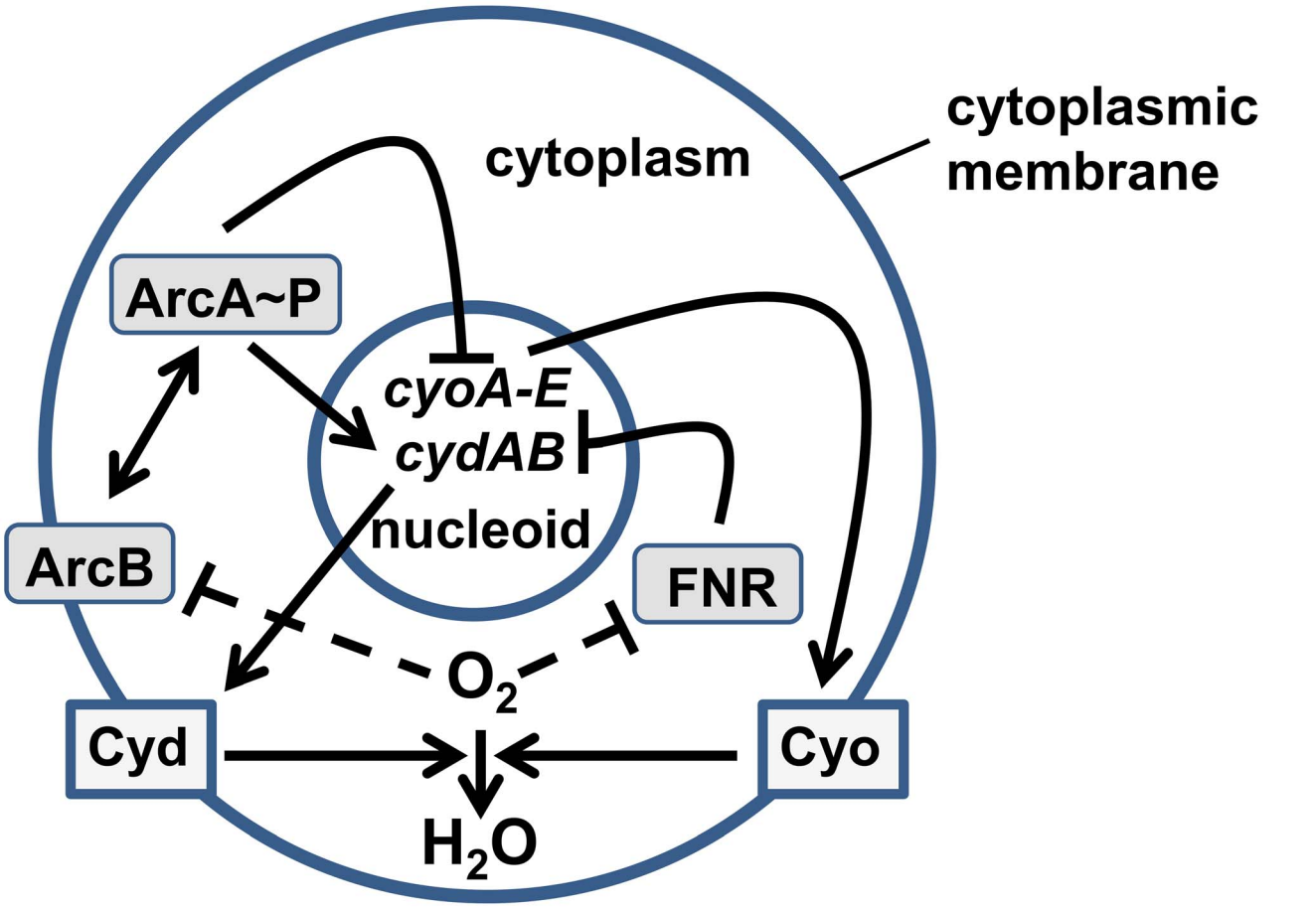

Figure 1. Components of the agent-based model. The diagram shows the interactions between and locations of the components of the model. Oxygen molecules (O_2) cross the cytoplasmic membrane and enter the bacterial cell where they are reduced to water (H_2O) by the action of the membrane-bound terminal oxidases (Cyo and Cyd). The transcription regulator, FNR is located in the cytoplasm and is inactivated by reaction with O_2. The active form of FNR represses the expression of both the *cydAB* and *cyoABCDE* operons located in the nucleoid. The ArcBA two-component system responds to O_2 indirectly (dashed line). The availability of O_2 alters the redox state of the electron transport chain and the production of fermentation products. These changes are sensed by the membrane-bound sensor ArcB, which autophosphorylates when O_2 is restricted. ArcB transfers phosphate to the cytoplasmic regulator ArcA, which acts to repress expression of *cyoABCDE* and activate expression of *cydAB*.
doi:10.1371/journal.pcbi.1003595.g001

Examination of the system as it transits from 0% to 217% AU showed that the DNA-bound, transcriptionally active FNR was initially protected from inactivation by consumption of O_2 at the cell membrane by the terminal oxidases and by reaction of O_2 with the iron-sulfur clusters of FNR dimers in the bacterial cytoplasm - the progress of this simulation is shown in Video S1. This new insight into the buffering of the FNR response could serve a useful biological purpose by preventing pre-mature switching off of anaerobic genes when the bacteria are exposed to low concentration O_2 pulses in the environment.

In the various niches occupied by *E. coli*, the bacterium can experience the full range of O_2 concentrations from zero, in the

Table 1. Numbers of Cyd, Cyo, ArcA and FNR molecules per *E. coli* cell at different points on the aerobiosis scale.

AU (%)	Cyd (molecules per cell)	Cyo (molecules per cell)	Total ArcA monomer (molecules per cell)	Total FNR monomer (molecules per cell)
0	11442	4336	8000	3000
31	51403	6202	8000	3000
85	66729	14017	8000	3000
115	19102	10985	8000	3000
217	10284	9036	8000	3000

The Cyd, Cyo and ArcA numbers are those reported by Rolfe et al. [3]. The number of FNR molecules per cell was calculated by from analysis of Western blots developed with anti-FNR serum for whole cell samples taken from steady-state cultures at the indicated aerobiosis units (AU).
doi:10.1371/journal.pcbi.1003595.t001

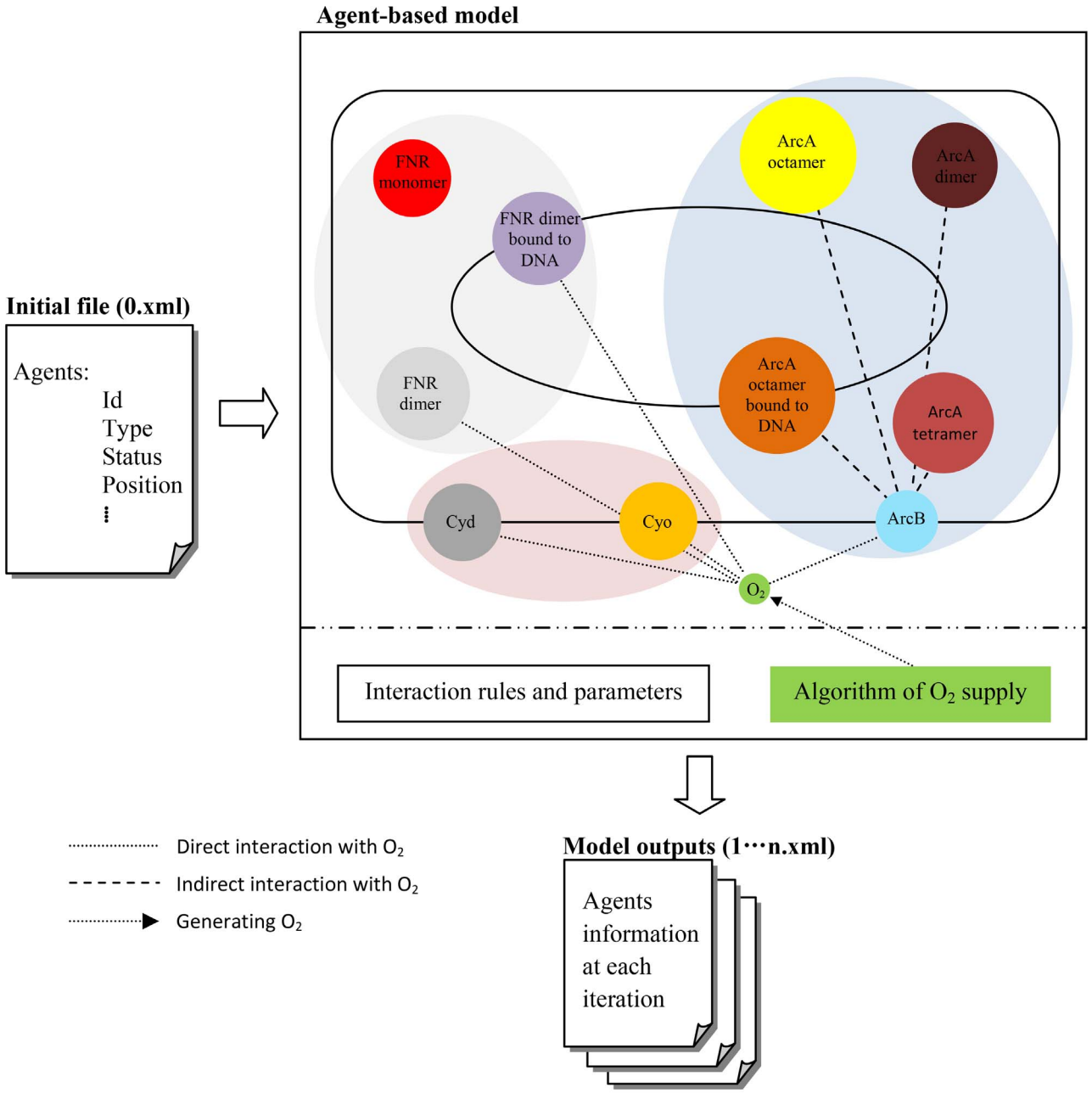

Figure 2. Components and process of agent-based model simulation. The file 0.xml contains all the settings for the agents involved to provide the initial model state. The FNR system, ArcBA system and terminal oxidases are displayed in light grey, light blue and light red ellipses respectively. The interaction rules and parameters are pre-defined, which determines how and when the interactions take place. For each of the iterations the number of O_2 molecules supplied to modelled cell is calculated. While model runs, updated information is generated in the same format as the initial file and stored in a series of xml files for further analysis. Experimental data, where available, were used for preparing the initial file and designing the interaction rules and parameters.
doi:10.1371/journal.pcbi.1003595.g002

anaerobic regions of a host alimentary tract, to full O_2 saturation (~200 μM, equivalent to ~120,000 O_2 molecules per cell), but fully aerobic metabolism is supported when the O_2 supply exceeds 1,000 O_2 molecules per cell. The profiles of five repetitive simulations for each agent in the model are presented in Figure 4. From iteration 1 to 5000 and iteration 15000 to 20000, O_2 was supplied at a constant value of ~6,500 molecules per cell such that the total number of O_2 molecules entering the cell increased linearly; when the O_2 supply was stopped (5000 to 15000 and 20000 to 30000 iterations) no more O_2 entered the cell and thus the number of O_2 molecules that had entered the cell remained unchanged during these periods (Figure 4a). When O_2 became available to the cell (from iteration 1), the sensor ArcB was de-phosphorylated and started to de-phosphorylate ArcA. Consequently, the number of ArcA octamers bound at their cognate sites in the nucleoid decreased rapidly. The ArcA tetramers and dimers produced during de-phosphorylation of the ArcA octamer were transformed to inactive (de-phosphorylated) ArcA dimers, (Figure 4d–f). Under aerobic conditions (iteration

Table 2. Agent properties.

Molecule	Form	Initial number	Step length (nm)	Initial location	Activity space
O_2	Molecule	0	Variable[1]	Outside the cell	From outside to inside of the cell
FNR	Monomer	0	15	n/a	Inside the cell
	Free dimer	1150	15	Evenly distributed in the cell	Inside the cell
	Dimer bound to DNA	350	0	Inside the nucleoid space	Stationary on DNA
ArcA[2]	Octamer	1000	18	Evenly distributed in the cell	Inside the cell
	Octamer bound to DNA	120	0	Inside the nucleoid space	Stationary on DNA
	Tetramer	0	10	n/a	Inside the cell
	Dimer	0	10	n/a	Inside the cell
ArcB[3]	Protein molecule	1000	5	Inner membrane	Inner membrane
Cyo	Oxidase molecule	Vary at different AU levels[4]	5	Inner membrane	Inner membrane
Cyd	Oxidase molecule	Vary at different AU levels[4]	5	Inner membrane	Inner membrane

The third column lists the number of molecules used to initiate the model.
[1]See Table 4.
[2]The ArcA numbers were reported by Rolfe et al. [3].
[3]The ArcB numbers are assumed based on the ~10:1 ratio of response-regulator to sensor-kinase for another *E. coli* two-component system PhoB-PhoR [22].
[4]Numbers are listed in Table 1.
doi:10.1371/journal.pcbi.1003595.t002

5000) all the ArcA was decomposed to inactive ArcA dimers. When the O_2 supply was stopped (from iteration 5001), the number of inactive ArcA dimers decreased rapidly as shown in Figure 4f, being transformed into phosphorylated ArcA dimers, tetramers and octamers (Figure 4c–e). Due to the phosphorylated ArcA dimers and tetramers combining to form ArcA octamers, their numbers dropped after initially increasing. The rate at which the ArcA octomers accumulated (ArcA activation) after O_2 withdrawal was slower than the rate of ArcA inactivation (Figures 4b and c). In this implementation of the modeled transition cycle, the numbers of

Table 3. Agent interaction rules.

Molecules	Interaction rules[1]
O_2	Interacting with FNR dimer, ArcB, Cyo and Cyd
FNR dimer	$FNR\ dimer + O_2 \xrightarrow{r_1=10} FNR\ monomer + FNR\ monomer$
	$FNR\ dimer + binding\ site \xrightarrow{r_2=5} FNR\ dimer\ bound\ to\ binding\ site$
FNR monomer	$FNR\ monomer + FNR\ monomer \xrightarrow{r_3=6} FNR\ dimer$
FNR dimer bound to DNA	$FNR\ dimer\ bound\ to\ binding\ site + O_2 \xrightarrow{r_4=10} FNR\ monomer + FNR\ monomer + unoccupied\ binding\ site$
ArcB	$ArcB{\sim}P + O_2 \xleftrightarrow{r_5=15} ArcB + O_2$
ArcA octamer	$ArcA\ octamer + ArcB \xrightarrow{r_6=35} ArcA\ tetramer + ArcA\ dimer{\sim}P + ArcA\ dimer + ArcB{\sim}P$
ArcA tetramer	$ArcA\ tetramer + ArcA\ tetramer \xrightarrow{r_7=3} ArcA\ octamer$
	$ArcA\ tetramer + ArcB \xrightarrow{r_8=35} ArcA\ dimer{\sim}P + ArcA\ dimer + ArcB{\sim}P$
ArcA dimer~P	$ArcA\ dimer{\sim}P + ArcA\ dimer{\sim}P \xrightarrow{r_9=3} ArcA\ tetramer$
	$ArcA\ dimer{\sim}P + ArcB \xleftrightarrow{r_{10}=35} ArcA\ dimer + ArcB{\sim}P$
ArcA dimer	$ArcA\ dimer + ArcB{\sim}P \xleftrightarrow{r_{11}=20} ArcA\ dimer{\sim}P + ArcB$
ArcA octamer bound to DNA	ArcA octamer bound to DNA is assigned a probability of 0.3% to leave the DNA in every iteration. This 'off rate' is required because ArcA~P dephosphorylation occurs by the action of ArcB at the cell membrane (see text).
Cyo	$Cyo + O_2 \xrightarrow{r_{12}=3} Cyo + H_2O$
Cyd	$Cyd + O_2 \xrightarrow{r_{13}=7} Cyd + H_2O$

The interaction radii (nm) were defined and refined as described in the *Methods*.
[1]Additional descriptions of the ArcBA and FNR interaction rules are provided in the *Supporting Information*.
doi:10.1371/journal.pcbi.1003595.t003

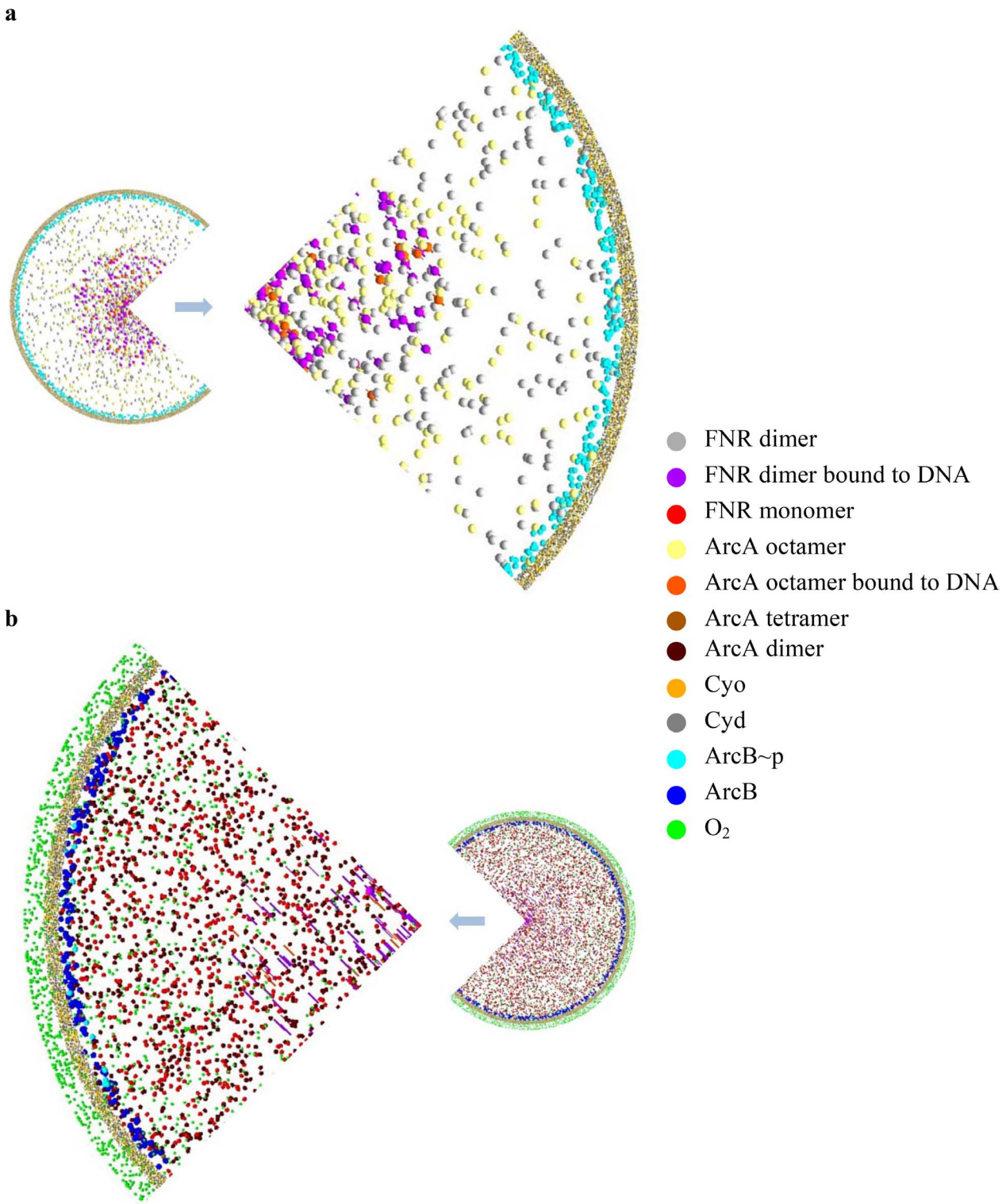

Figure 3. The initial and final states of model with no O_2 and with excess O_2 supplied. (a) The initial state of model with no O_2 (0% AU) supplied to the cell. (b) The final state of model with excess O_2 (217%) supplied to the cell. Each type of molecule is represented by a different color as shown in the key.
doi:10.1371/journal.pcbi.1003595.g003

ArcA octamers in the cytoplasm and bound to DNA did not reach that observed in the initial state before the second cycle of O_2 supply began, indicating that a longer period is required to return to the fermentation state.

The numbers of FNR dimer bound to binding sites and free FNR dimer (cytoplasmic FNR dimer) decreased when O_2 was supplied to the system (Figures 4g–h), but the rate was slower than that for ArcA inactivation, consistent with O_2 consumption at the

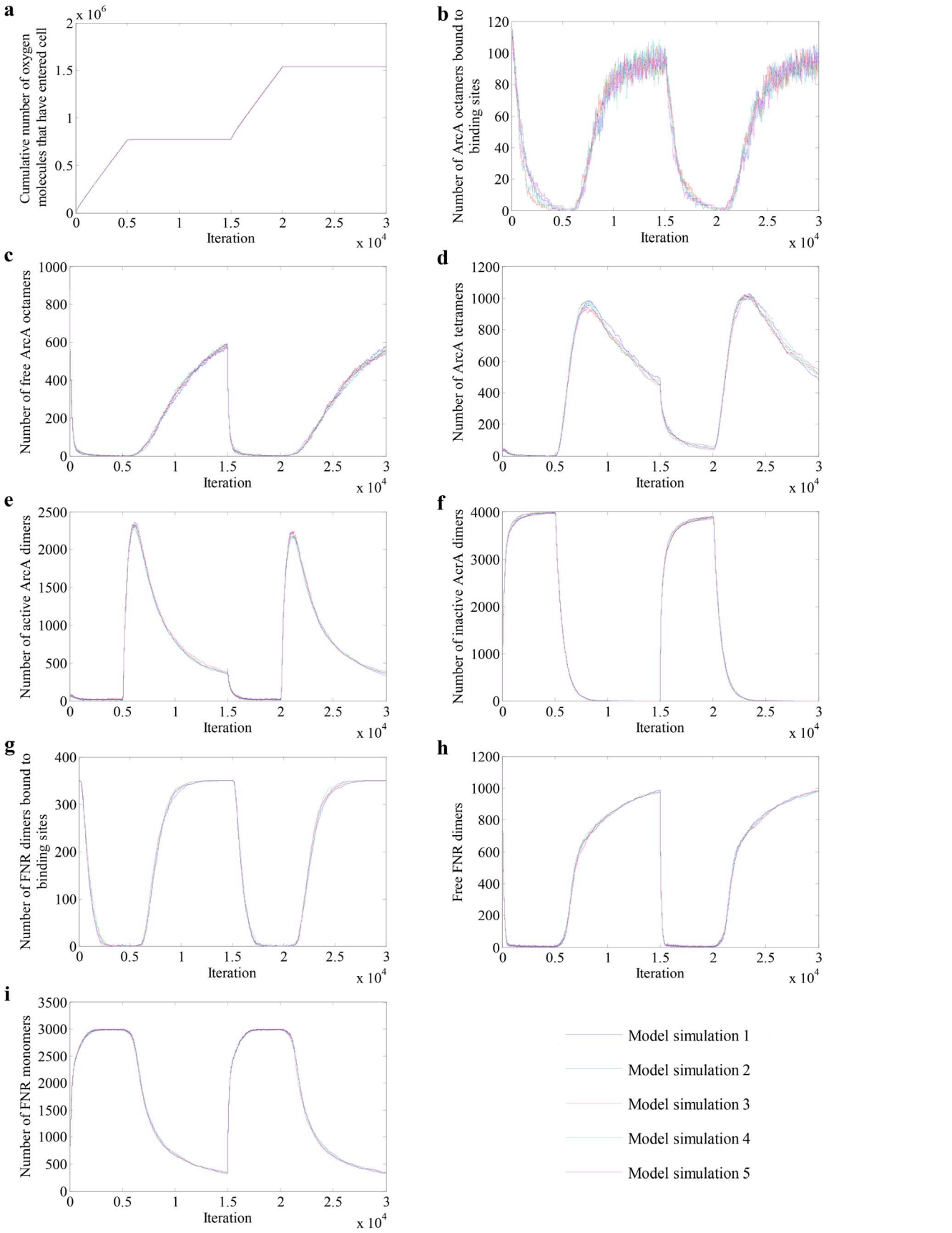
a
Cumulative number of oxygen molecules that have entered cell
x 10^6
Iteration
x 10^4
b
Number of ArcA octamers bound to binding sites
Iteration
x 10^4
c
Number of free ArcA octamers
Iteration
x 10^4
d
Number of ArcA tetramers
Iteration
x 10^4
e
Number of active ArcA dimers
Iteration
x 10^4
f
Number of inactive AcrA dimers
Iteration
x 10^4
g
Number of FNR dimers bound to binding sites
Iteration
x 10^4
h
Free FNR dimers
Iteration
x 10^4
i
Number of FNR monomers
Iteration
x 10^4
Model simulation 1
Model simulation 2
Model simulation 3
Model simulation 4
Model simulation 5

Figure 4. Model simulation output: quantitative variation of ArcA and FNR molecules in response to O_2 availabilities. (a) Cumulative number of O_2 molecules that have entered the modeled cell. (b–f) The changes in the numbers of ArcA octamers bound to DNA, free ArcA octamers, ArcA tetramers, active (phosphorylated) ArcA dimers, and inactive (de-phosphorylated) ArcA dimers. (g–i) The profiles of FNR dimers bound to DNA, free FNR dimers and FNR monomers. The data were taken from 5 repeats of model simulation with 30,000 iterations per run.
doi:10.1371/journal.pcbi.1003595.g004

membrane, which can be sensed by ArcB to initiate inactivation of ArcA, but lowers the signal for inactivation of FNR. When O_2 was removed from the system (from iteration 5001) FNR was activated over a similar timeframe to ArcA (Figures 4b and g), which was again consistent with previous observations [15]. As with ArcA, free FNR dimers and FNR monomers did not fully return to their initial states after O_2 supply was withdrawn in the model, indicating that further iterations are required to reach steady-state (Figure 4h–i). These results clearly indicate that the model is self-adaptive to the changes in O_2 availability, and the reproducible responses prove the reliability and robustness of the model. The ArcBA system simulated in this model is based on a preliminary biological assumption, and the agent-based model presented here should prove a reliable and flexible platform for exploring the key components of the system and testing new experimental findings.

Model validation

In order to validate the model with biological measurements of FNR DNA-binding activity estimated using an FNR-dependent *lacZ* reporter, the ArcBA system agents were removed from the model by setting their agent numbers to zero. The ArcBA system is an indirect O_2 sensor and does not consume O_2, hence the FNR system was not affected by withdrawing ArcBA from the model, but this simplification increased simulation speed.

The O_2 step length and other model parameters were estimated using the experimental data obtained at 31% AU. Using the estimated O_2 step length at 31% AU and defining the step length of O_2 molecule, S_{O_2}, as 0 at 0% AU, a linear model, $S_{O_2} = k \times C_{O_2}$, was constructed to predict the step lengths of O_2 at other AU levels, where $k = 2.1$ and C_{O_2} represents the O_2 concentration at different AU levels (Table 4). The O_2 step lengths predicted by this model were used to validate the model at 85%, 115% and 217% AU, and the accuracy of the linear model was shown by the good correlation between the model and experimental data.

Profiles of five repetitive simulations in which the simplified model was used to predict the numbers of active FNR dimers in steady-state cultures of bacteria grown at different AU values are presented in Figure 5. At 31% AU, the model implied that FNR-mediated gene expression is unaffected compared to an anaerobic culture (0% AU), i.e. the number of FNR binding sites occupied in the nucleoid remained unchanged (Figures 5a and e). Even at 85% AU, ~80% of the FNR-binding sites remained occupied (Figures 5b and f). It was only when the O_2 supply was equivalent to >115% AU that occupation of the FNR-binding sites in the nucleoid decreased (Figures 5 c, d, g and h). These outputs matched the FNR activities calculated from the measurements of an FNR-dependent reporter (Table 5) and thus demonstrate the abilities of the model to simulate the general behavior of FNR dimers in steady-state cultures of *E. coli*.

A second validation approach using two FNR variants that are compromised in their ability to undergo monomer-dimer transitions was adopted. The FNR variant FNR I151A can acquire an iron-sufur cluster in the absence of O_2, but subsequent dimerization is impaired [26]. The FNR D154A variant can also acquire an iron-sulfur cluster under anaerobic conditions, but does not form monomers in the presence of O_2 [26]. To mimic the behavior of these two FNR variants the interaction radius for FNR dimer formation was changed in the model. Thus, the interaction distance for wild-type FNR monomers, which was initially set at 6 nm (r_3, Table 3) was increased to 2000 nm for the FNR D154A variant, essentially fixing the protein as a dimer, or decreased to 2.5 nm for the FNR I151A variant, making this protein predominantly monomeric under anaerobic conditions. The results of simulations run under aerobic (217% aerobiosis) and anaerobic conditions (0% aerobiosis) suggested that under aerobic conditions wild-type FNR and FNR I151A should be unable to inhibit transcription from an FNR-repressed promoter (i.e. the output from the reporter system is 100%), whereas FNR D154A should retain ~50% activity (Table 6). Under anaerobic conditions, wild-type FNR was predicted to exhibit maximum repressive activity (i.e. 0% reporter output), whereas FNR I151A and FNR D154A mediated slightly enhanced repression compared to the simulated aerobic conditions (Table 6). To test the accuracy of these predictions, the ability of wild-type FNR, FNR I151A and FNR D154A to repress transcription of a synthetic FNR-regulated promoter (*FFgalΔ4*) under aerobic and anaerobic conditions was tested [27]. The choice of a synthetic FNR-repressed promoter was made to remove complications that might arise due to iron-sulfur cluster incorporation influencing the protein-protein interactions between FNR and RNA polymerase; in the reporter system chosen FNR simply occludes the promoter of the reporter gene and as such DNA-binding by FNR controls promoter

Table 4. Relative parameters for O_2 molecules.

AU (%)	O_2 in input gas (%)	O_2 molecules per cell per iteration	Step length of O_2 molecule (nm)
0	0	0	0
31	2.8	13	6
85	8.1	37	14.5±2.5
115	11.1	51	25.5±0.5
217	21.1	97	41.5±1.5

The percentages of O_2 in the input gas at different AU levels (first column) are listed in the second column. The third column presents the calculated numbers of O_2 molecules supplied to a cell. The step length values are listed in the fourth column are obtained from a set of model tests at 31% AU only and were validated at 85%, 115% and 217% AU.
doi:10.1371/journal.pcbi.1003595.t004

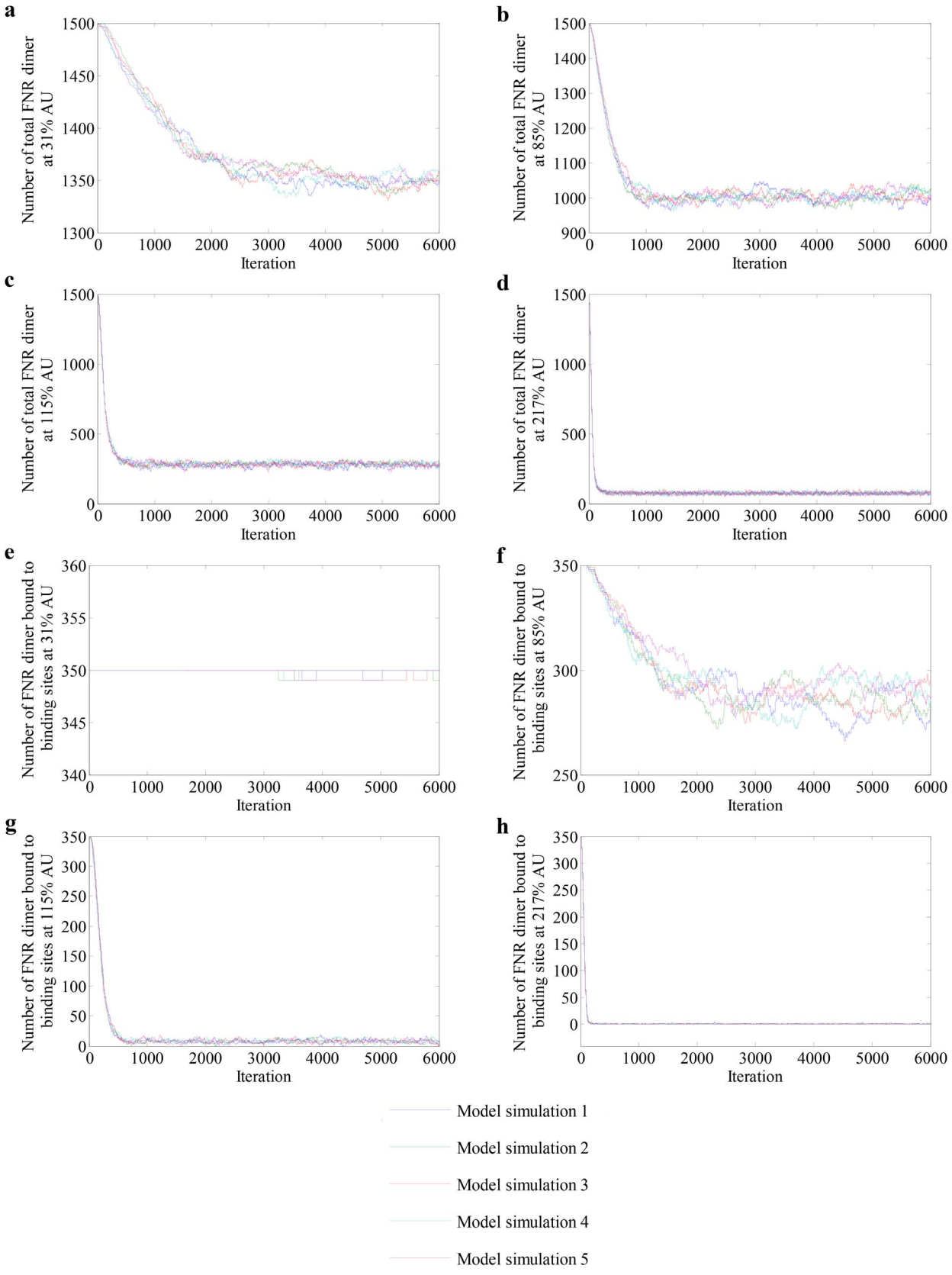

Figure 5. Profiles of FNR dimers at different AU levels. (a–d) Variation of the numbers of total FNR dimers and (e–h) numbers of FNR dimers bound to DNA at AU levels 31%, 85%, 115% and 217% respectively.
doi:10.1371/journal.pcbi.1003595.g005

Table 5. Comparison between experimental and simulation results for wild-type FNR.

	Simulation results			Experimental results	
Aerobiosis units (%)	**Total FNR dimer (molecules per cell)**	**FNR dimer bound to binding sites (molecules per cell)**	**Predicted output from an FNR-dependent promoter (% of maximum)**	**Total FNR dimer (molecules per cell)[1]**	**Measured output from an FNR-dependent promoter (% of maximum)[2]**
0	1500	350	100	1500	100±3
31	1350±6	350	100	1377	95±4
85	1033±16	287±16	82±4.6	1020	67±7
115	280±15	7±3	2±0.9	248	13±3
217	73±8	0	0	60	0

The model simulation data was taken by averaging the model outputs at steady-state. For these results, the values shown are the averages and standard deviations. The last column shows experimentally determined transcription from the FNR-dependent *FF-41.5-lacZ* promoter; the transcriptional output at 0% AU was set to 100.
[1]The total numbers of FNR dimers were calculated from the Western blots and FNR-dependent promoter activities.
[2]The measured output from an FNR-dependent promoter was reported by [15,38].
doi:10.1371/journal.pcbi.1003595.t005

activity. The experimental data obtained matched the general response of the FNR variants in the simulation, but not very precisely for FNR D154A, with the experimental data indicating more severe repression by FNR D154A under both aerobic and anaerobic conditions than predicted (Table 6). This suggested that the interaction radius ($r_2 = 5$ nm; Table 3), which controls the binding of FNR to its DNA target required adjustment to enhance DNA-binding of the FNR D154A variant. Therefore, the simulations were rerun after adjusting r_2 to 7 nm for all the FNR proteins considered here. The results of the simulations for both FNR variants now matched the experimental data well (Table 6). However, it was essential to ensure that the adjustment to r_2 did not significantly influence the model output for wild-type FNR. Therefore, simulations of the behaviour of wild-type FNR at 31, 85, 115 and 217% aerobiosis were repeated using the adjusted r_2 value of 7 nm. The model output was very similar to those obtained when r_2 was at the initial value of 5 nm (Table 7). These analyses imply that for FNR D154A, which is essentially fixed in a dimeric state, the rate of binding to the target DNA governs transcriptional repression, but for wild-type FNR the upstream monomer-dimer transition is the primary determinant controlling the output from the reporter.

Concluding remarks

The FNR switch has been the subject of several attempts to integrate extensive experimental data into coherent models that account for changes in FNR activity and target gene regulation in response to O_2 availability [15,28–31]. These models have provided estimates of active and inactive FNR in *E. coli* cells exposed to different O_2 concentrations and the dynamic behavior of the FNR switch. The ability of FNR to switch rapidly between active and inactive forms is essential for it to fulfill its physiological role as a global regulator and the models are able to capture this dynamic behavior. Thus, it is thought that the 'futile' cycling of FNR between inactive and active forms under aerobic conditions has evolved to facilitate rapid activation of FNR upon withdrawal of O_2 and hence the physiological imperative for rapid activation has determined the structure of the FNR regulatory cycle [30,31]. However, it is less clear from these approaches how the system avoids undesirable switching between active and inactive states at low O_2 availabilities (micro-aerobic conditions, >0%–<100% AU). To achieve rapid FNR response times it has been suggested that minimizing the range of O_2 concentrations that constitute a micro-aerobic environment, from the viewpoint of FNR, is advantageous [31]. Unlike previous models of the FNR switch,

Table 6. Comparison between experimental and simulation results for FNR variants.

Expression from an FNR-repressed promoter (%)						
Strain	**Aerobic**			**Anaerobic**		
	Simulation ($r_3 = 5$ nm)[1]	**Experiment[2]**	**Simulation ($r_3 = 7$ nm)**	**Simulation ($r_3 = 5$ nm)**	**Experiment**	**Simulation ($r_3 = 7$ nm)**
FNR	100	108.2±2.2	99.7	0	13.0±1.2	0
FNR I151A	100	126.7±2.8	100	87.5±1.4	83.3±4.4	79.6±0.7
FNR D154A	52.0±1.2	26.2±1.2	30.4±0.6	52.0±2.1	32.6±3	31.5±1.3

[1]For the simulations, the standard deviations were calculated from 5 repeats for FNR and 13 repeats for FNR I151A and FNR D154A. The aerobic condition in simulation was modelled at AU level 217%, and the anaerobic condition was modelled at AU level 0%. r_3 is the interaction radius between the FNR dimer and its cognate DNA-binding site.
[2]For the experimental data 100% expression was set as the β-galactosidase activity obtained in the absence of FNR. Measurements were made from three independent cultures.
doi:10.1371/journal.pcbi.1003595.t006

Table 7. The effect of interaction distance (r_3) for binding of FNR dimers to target DNA on wild-type FNR activity.

	FNR dimer bound to binding sites (% of maximum)			
Interaction radius	**31% AU**	**85% AU**	**115% AU**	**217% AU**
$r_3 = 5$ nm[1]	100	82±4.6	2±0.9	0
$r_3 = 7$ nm	100	89.8±0.7	4.5±0.6	0.3

The standard deviations for $r_3 = 5$ nm were obtained from 5 repeats and for $r_3 = 7$ nm 10 repeats of the simulation.
[1]r_3 is the interaction radius between the FNR dimer and its cognate DNA-binding site.
doi:10.1371/journal.pcbi.1003595.t007

the agent-based model described here recognizes the importance of geometry and location in biology. This new approach reveals that spatial effects play a role in controlling the inactivation of FNR in low O_2 environments. Consumption of O_2 by terminal oxidases at the cytoplasmic membrane and reaction of O_2 with the iron-sulfur clusters of FNR in the cytoplasm present two barriers to inactivation of FNR bound to DNA in the nucleoid, thereby minimizing exposure of FNR to micro-aerobic conditions by maintaining an essentially anaerobic cytoplasm for AU values up to ~85%. It is suggested that this buffering of FNR response makes the regulatory system more robust by preventing large amplitude fluctuations in FNR activity when the bacteria are exposed to micro-aerobic conditions or experience environments in which they encounter short pulses of low O_2 concentrations. Furthermore, investigation of FNR variants with altered oligomerization properties suggested that the monomer-dimer transition, mediated by iron-sulfur cluster acquisition, is the primary regulatory step in FNR-mediated repression of gene expression. It is expected that the current model will act as a foundation for future investigations, e.g. predicting the effects of adding or removing a class of agent to identify the significant regulatory components of the system.

Methods

Measurement of the rate of O_2 supply

Knowledge of the rate of O_2 supply, R_{O_2}, to the *E. coli* cells was required in order to simulate the response of the regulators of *cydAB* and *cyoABCDE* to different O_2 availabilities. Therefore, uninoculated chemostat vessels were used to measure dissolved O_2 concentrations, D_{O_2}, as a function of the percentage O_2 in the input gas, P_i, in the absence of bacteria. This allowed the rate at which O_2 dissolves in the culture medium to be calculated from the equation: $D_{O_2} = R_{O_2} \times P_i$, yielding $R_{O_2} = 5.898$ µmol/L/min. The number of O_2 molecules distributed to a single bacterial cell was then calculated from the following equation: $Num_{O_2} = D_{O_2} \times N_A \times V_{cell} \times n$ (where, N_A is the Avogadro constant (6.022×10^{23}), V_{cell} is the volume of *E. coli* cell (0.3925 µm^3) and as a constant for this equation, n (3.3×10^{-9}) includes the unit transformations, min to sec (60^{-1}) and µmol to mol (10^{-6}), and the time unit represented by an iteration (0.2 sec).

Control of agent mobility

In the model the individual agents (Cyd, Cyo, ArcB, ArcA, FNR and O_2) are able to move and interact within the confines of their respective locations in a 3-D-cylinder representing the *E. coli* cell. To control the velocity of agents, the maximal distances they can move in 3-D space during one iteration (step length) were pre-defined (Table 4). Thus, a step length is pre-defined in program header file (.h) and for each movement, this is multiplied by a randomly generated value within [0,1] to obtain a random moving distance, which in turn is directed towards a 3-D direction (movement vector) that was also randomly generated within defined spatial regions. An example is shown in Figure 6 to illustrate the movements of an O_2 molecule when it enters the cell.

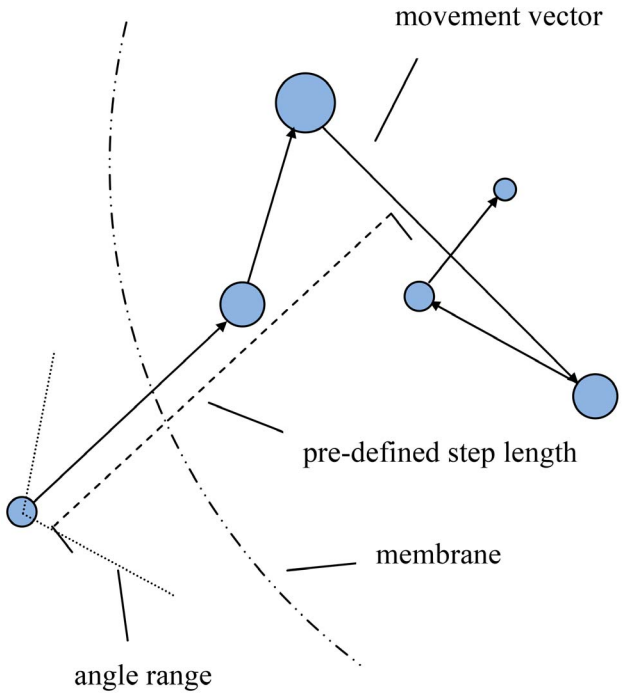

Figure 6. The 3-D movement of an O_2 molecule during five successive iterations. Within a pre-defined limit (step length) the agent moves a random distance per iteration. For O_2 this is also used to imitate the diffusion along the concentration gradient according to Fick's first law, in which the flux goes from regions of high concentration to regions of low concentration with a magnitude that is proportional to the concentration gradient (spatial derivative). The adjustment of step length of O_2 (Table 4) affects the spatial moving speed, which is simply represented as the greater the step length, the faster the movement. The angle range was defined for O_2 molecules that are outside the cell to enable them move towards cell. The O_2 molecules inside the cell and all other molecules move in any direction within their defined spatial regions.
doi:10.1371/journal.pcbi.1003595.g006

Estimating interaction radii

Interactions between agents depend upon the biological rules governing their properties and being in close enough proximity to react. The interaction radius of an agent encapsulates the 3-D space within which reactions occur. As the interaction radii cannot be measured, they were first estimated on the basis of known biological properties. For the radii $r_{1\ldots4}$, r_{12} and r_{13} (Table 3), arbitrary values were initially set at 31% AU, and the model was then trained to match the experimental result for the number of FNR dimers at 31% AU (Table 5). The modeled output of FNR dimer number at steady-state was compared with the experimental data, and the difference suggested re-adjustment of interaction radii. The adjusted radii were then tested against the FNR dimer numbers at 85%, 115% and 217% AU (Table 5) during model validation, and the results indicate that the interaction radii values are capable of describing the behavior of the system. The

interaction radii of Cyd and Cyo with O_2 reflect their relative affinities for O_2 (i.e. Cyd has a high O_2 affinity and thus reacts more readily, 7 nm interaction radius, than Cyo, which has a lower affinity for O_2, 3 nm interaction radius). As, thus far, no accurate biological data is available for ArcBA system, the radii $r_{5\ldots11}$ were arbitrarily defined and were refined by training the model to match current biological expectations.

Model description

The rod-shaped *E. coli* cell was modeled as a cylinder (500 nm×2000 nm) [32] with the nucleoid represented as a sphere with a diameter of 250 nm at the centre of the cell. The experimentally-based parameters and locations of the agents in their initial state are listed in Table 2. As the number of ArcB molecules has not been determined experimentally, this value was arbitrarily assigned (see above). The interaction rules for the agents are shown in Table 3 (additional descriptions of an exemplar agent (O_2) and the rules for ArcBA and FNR are provided in Figure S1, Table S1 and Text S1). These rules, combined with the interaction radii, determine the final status of the system. The scale of the model is such that high performance computers are required to implement it, and the flexible agent-based supercomputing framework, FLAME (http://www.flame.ac.uk) acted as the framework to enable the simulation [33,34]. For more information on FLAME see Figure S2 and Text S2.

Measurement of the activities of FNR and FNR variants *in vivo*

Plasmids encoding the FNR variants were constructed by site-directed mutagenesis (Quikchange, Agilent) of pGS196, which contains a 5.65 kb fragment of wild-type *fnr* ligated into pBR322 [35]. The three isogenic plasmids pGS196 (FNR), pGS2483 (FNR I151A) and pGS2405 (FNR D154A) were used to transform *E. coli* JRG4642 (an *fnr lac* mutant strain) containing a pRW50-based reporter plasmid carrying the *lac*-operon under the control of the *FFgal*Δ*4* promoter [27].

β-Galactosidase assays were carried out as described previously on strains grown in LBK medium at pH 7.2 containing 20 mM glucose [36,37]. Cultures were grown either aerobically (25 ml culture in a 250 ml flask at 250 rpm agitation with 1:100 inoculation) or anaerobically (statically in a fully sealed 17 ml tube with 1:50 inoculation). Cultures (three biological replicates) were grown until mid-exponential phase ($OD_{600} = 0.35$) before assaying for β-galactosidase activity.

Supporting Information

Figure S1 Stategraph for O_2 molecules. In order to describe the model clearly, every agent is given a formal description to illustrate its states, memory, functions, and relevant messages that it sends out or receives from other agents (see Table S1). The stategraph for an oxygen agent is shown in the diagram.
(TIFF)

Figure S2 Building a FLAME simulation file. The agent definition (written in XMML) is parsed by a FLAME model parser, called *xparser*, which generates the simulation code. In the GCC environment, the code is compiled with the message board library, *libmboard*. The initial agent population settings are set in 0.xml file as the starting status of the model.
(TIFF)

Table S1 Agent description for the O_2 molecule.
(DOCX)

Text S1 Additional description of interaction rules for the regulatory systems, ArcBA and FNR.
(DOCX)

Text S2 The agent-based modeling framework: FLAME.
(DOCX)

Video S1 Simulation of ArcBA and FNR activities in response to O_2 over two 0–217% AU cycles.
(MP4)

Acknowledgments

The authors thank Afsaneh Maleki-Dizaji for initializing the model structure, Melanie Stapleton for pGS2405 and the other members of the SysMo-SUMO$_2$ consortium for many useful discussions: M. Ederer, D. Knies, O. Sawodny, G. Sanguinetti, B. Cseke, K. Bettenbrock, S. Stagge, S. Steinsiek, P. Sharma, F. Bruggeman and J. Teixeira de Mattos.

Author Contributions

Conceived and designed the experiments: HB MDR WJ RKP JG MH. Performed the experiments: HB MDR. Analyzed the data: HB MDR. Contributed reagents/materials/analysis tools: SC. Wrote the paper: HB WJ JG MH.

References

1. Gennis RB, Stewart V (1996) Respiration, in *Escherichia coli* and Salmonella Cellular and Molecular Biology: ASM Press, Washington DC. 217–261 p.
2. Trumpower BL, Gennis RB (1994) Energy transduction by cytochrome complexes in mitochondrial and bacterial respiration: the enzymology of coupling electron transfer reactions to transmembrane proton translocation. Annu Rev Biochem 63: 675–716.
3. Rolfe MD, Ter Beek A, Graham AI, Trotter EW, Asif HM, et al. (2011) Transcript profiling and inference of *Escherichia coli* K-12 ArcA activity across the range of physiologically relevant oxygen concentrations. J Biol Chem 286: 10147–10154.
4. D'Mello R, Hill S, Poole RK (1995) The oxygen affinity of cytochrome *bo′* in *Escherichia coli* determined by the deoxygenation of oxyleghemoglobin and oxymyoglobin: K_m values for oxygen are in the submicromolar range. J Bacteriol 177: 867–870.
5. D'Mello R, Hill S, Poole RK (1996) The cytochrome *bd* quinol oxidase in *Escherichia coli* has an extremely high oxygen affinity and two oxygen-binding haems: implications for regulation of activity in vivo by oxygen inhibition. Microbiology 142: 755–763.
6. Stolper DA, Revsbech NP, Canfield DE (2010) Aerobic growth at nanomolar oxygen concentrations. Proc Natl Acad Sci U S A 107: 18755–18760.
7. Cotter PA, Gunsalus RP (1992) Contribution of the *fnr* and *arcA* gene products in coordinate regulation of cytochrome *o* and *d* oxidase (*cyoABCDE* and *cydAB*) genes in *Escherichia coli*. FEMS Microbiol Lett 70: 31–36.
8. Crack JC, Green J, Thomson AJ, Le Brun NE (2012) Iron-sulfur cluster sensor-regulators. Curr Opin Chem Biol 16: 35–44.
9. Crack JC, Green J, Cheesman MR, Le Brun NE, Thomson AJ (2007) Superoxide-mediated amplification of the oxygen-induced switch from [4Fe-4S] to [2Fe-2S] clusters in the transcriptional regulator FNR. Proc Natl Acad Sci U S A 104: 2092–2097.
10. Crack JC, Green J, Hutchings MI, Thomson AJ, Le Brun NE (2012) Bacterial iron-sulfur regulatory proteins as biological sensor-switches. Antioxid Redox Signal 17: 1215–1231.
11. Constantinidou C, Hobman JL, Griffiths L, Patel MD, Penn CW, et al. (2006) A reassessment of the FNR regulon and transcriptomic analysis of the effects of nitrate, nitrite, NarXL, and NarQP as *Escherichia coli* K12 adapts from aerobic to anaerobic growth. J Biol Chem 281: 4802–4815.
12. Salmon K, Hung SP, Mekjian K, Baldi P, Hatfield GW, et al. (2003) Global gene expression profiling in *Escherichia coli* K12. The effects of oxygen availability and FNR. J Biol Chem 278: 29837–29855.
13. Kang Y, Weber KD, Qiu Y, Kiley PJ, Blattner FR (2005) Genome-wide expression analysis indicates that FNR of *Escherichia coli* K-12 regulates a large number of genes of unknown function. J Bacteriol 187: 1135–1160.
14. Iuchi S, Lin EC (1991) Adaptation of *Escherichia coli* to respiratory conditions: regulation of gene expression. Cell 66: 5–7.
15. Rolfe MD, Ocone A, Stapleton MR, Hall S, Trotter EW, et al. (2012) Systems analysis of transcription factor activities in environments with stable and dynamic oxygen concentrations. Open Biol 2: 120091.

16. Georgellis D, Kwon O, Lin EC (2001) Quinones as the redox signal for the arc two-component system of bacteria. Science 292: 2314–2316.
17. Salmon KA, Hung SP, Steffen NR, Krupp R, Baldi P, et al. (2005) Global gene expression profiling in *Escherichia coli* K12: effects of oxygen availability and ArcA. J Biol Chem 280: 15084–15096.
18. Liu X, De Wulf P (2004) Probing the ArcA-P modulon of *Escherichia coli* by whole genome transcriptional analysis and sequence recognition profiling. J Biol Chem 279: 12588–12597.
19. Becker S, Holighaus G, Gabrielczyk T, Unden G (1996) O_2 as the regulatory signal for FNR-dependent gene regulation in *Escherichia coli*. J Bacteriol 178: 4515–4521.
20. Marshall FA, Messenger SL, Wyborn NR, Guest JR, Wing H, et al. (2001) A novel promoter architecture for microaerobic activation by the anaerobic transcription factor FNR. Mol Microbiol 39: 747–753.
21. Alexeeva S, Hellingwerf KJ, Teixeira de Mattos MJ (2002) Quantitative assessment of oxygen availability: perceived aerobiosis and its effect on flux distribution in the respiratory chain of *Escherichia coli*. J Bacteriol 184: 1402–1406.
22. Gao R, Stock AM (2013) Probing kinase and phosphatase activities of two-component systems *in vivo* with concentration-dependent phosphorylation profiling. Proc Natl Acad Sci U S A 110: 672–677.
23. Myers KS, Yan H, Ong IM, Chung D, Liang K, et al. (2013) Genome-scale analysis of *Escherichia coli* FNR reveals complex features of transcription factor binding. PLoS Genet 9: e1003565.
24. Grainger DC, Aiba H, Hurd D, Browning DF, Busby SJ (2007) Transcription factor distribution in *Escherichia coli*: studies with FNR protein. Nucleic Acids Res 35: 269–278.
25. Robison K, McGuire AM, Church GM (1998) A comprehensive library of DNA-binding site matrices for 55 proteins applied to the complete *Escherichia coli* K-12 genome. J Mol Biol 284: 241–254.
26. Moore LJ, Mettert EL, Kiley PJ (2006) Regulation of FNR dimerization by subunit charge repulsion. J Biol Chem 281: 33268–33275.
27. Williams SM, Wing HJ, Busby SJW (1998) Repression of transcription initiation by the *Escherichia coli* FNR protein: repression by FNR can be simple. FEMS Microbiol Lett 163: 203–208.
28. Partridge JD, Sanguinetti G, Dibden DP, Roberts RE, Poole RK, et al. (2007) Transition of *Escherichia coli* from aerobic to micro-aerobic conditions involves fast and slow reacting components. J Biol Chem 282:11230–11237.
29. Peercy BE, Cox SJ, Shalel-Levanon S, San K-Y, Bennett G (2006) A kinetic model of oxygen regulation of cytochrome production in *Escherichia coli*. J Theoretical Biol 242: 547–563.
30. Tolla DA, Savageau MA (2010) Regulation of aerobic-to-anaerobic transitions by the FNR cycle in *Escherichia coli*. J Mol Biol 397: 893–905.
31. Tolla DA, Savageau MA (2011) Phenotypic repertoire of the FNR regulatory network in *Escherichia coli*. Mol Microbiol 79: 149–165.
32. Nelson DE, Young KD (2000) Penicillin binding protein 5 affects cell diameter, contour, and morphology of *Escherichia coli*. J Bacteriol 182: 1714–1721.
33. Greenough C, Worth D, Chin S, Holcombe M, Coakley S (2008) The exploitation of parallel high performance systems in the FLAME agent-based simulation framework. RAL Technical Reports RAL-TR-2008–022.
34. Richmond P, Walker D, Coakley S, Romano D (2010) High performance cellular level agent-based simulation with FLAME for the GPU. Brief Bioinform 11: 334–347.
35. Spiro S, Guest JR (1988) Inactivation of the FNR protein of *Escherichia coli* by targeted mutagenesis in the N-terminal region. Mol Microbiol 2: 701–707.
36. Miller JH 1972. Assay of β-galactosidase. In *Experiments in molecular genetics* (ed. Miller JH), pp. 352–355 New York, NY: Cold Spring Harbor Laboratory.
37. Wyborn NR, Messenger SL, Henderson RA, Sawers G, Roberts RE, et al. (2002) Expression of the *Escherichia coli yfiD* gene responds to intracellualr pH and reduces the accumulation of acidic metabolic end products. Microbiology 148: 1015–1026.
38. Jervis AJ, Green J (2007) *In vivo* demonstration of FNR dimers in response to lower O_2 availability. J Bacteriol 189: 2930–2932.